Experimental Demonstration of Thermal Chameleonlike Rotators with Transformation-Invariant Metamaterials

Fubao Yang, Boyan Tian, Liujun Xu,* and Jiping Huang†
Department of Physics, State Key Laboratory of Surface Physics, and Key Laboratory of Micro and Nano Photonic Structures (MOE), Fudan University, Shanghai 200438, China

(Received 31 August 2020; revised 16 September 2020; accepted 21 October 2020; published 11 November 2020)

Intelligent metamaterials have aroused intensive research interest due to their adaptive responses to environmental changes. However, existing transformation-thermotics-based metamaterials have almost no intelligence because their parameters are crucially dependent on environmental parameters. Therefore, once the environment changes, these thermal metamaterials can no longer work, which limits practical applications. To solve the problem, we propose a mechanism for intelligent thermal metamaterials based on transformation-invariant metamaterials. As an application, we design intelligent thermal rotators, which can guide the direction of heat flux with different environmental parameters. Since the adaptive behavior is similar to chameleons, the present rotators are also called chameleonlike rotators. We further perform finite-element simulations and laboratory experiments to validate the scheme, and the chameleonlike behavior is clearly demonstrated. These results have potential applications for the implementation of adaptive and adjustable thermal metamaterials. Similar behaviors can also be expected in other fields like hydrodynamics.

DOI: 10.1103/PhysRevApplied.14.054024

I. INTRODUCTION

Transformation thermotics [1,2] provides a fundamental and powerful method to control heat flux at will. Initial explorations mainly focused on thermal conduction, and lots of functions were proposed such as cloaking, concentrating, and rotating [3]. For the sake of practical applications, convection [4–6] and radiation [7,8] have also been considered to develop corresponding transformation theories.

Although transformation-thermotics-based metamaterials have achieved great success, the lack of intelligence remains a problem. Concretely speaking, the key equation of transformation thermotics is $\overleftrightarrow{\kappa}' = \mathbf{J}\,\overleftrightarrow{\kappa}\,\mathbf{J}^{\tau}/\det\mathbf{J}$, where $\overleftrightarrow{\kappa}'$ is transformed thermal conductivity, $\overleftrightarrow{\kappa}$ is environmental thermal conductivity, $\mathbf{J}$ is the Jacobian matrix, and τ denotes transpose [1,2]. Clearly, the transformed parameter $\left(\overleftrightarrow{\kappa}'\right)$ is crucially dependent on the environmental parameter $\left(\overleftrightarrow{\kappa}\right)$. In other words, once the environment changes, the transformed parameter should change accordingly, which makes the original design fail in the new environment. This limitation is fatal because one device is applicable for only one environment. Similar problems also exist in the fields of electromagnetism and thermal radiation, and some inspiring studies [9,10] gave insights.

To improve the intelligence of thermal metamaterials, here we propose a mechanism based on thermal transformation-invariant metamaterials [11,12], whose thermal conductivities are highly anisotropic [13–15], i.e., $0\,\mathrm{W\,m^{-1}\,K^{-1}}$ for one direction and $\infty\,\mathrm{W\,m^{-1}\,K^{-1}}$ for the other. Actually, transformation-invariant (i.e., highly anisotropic) metamaterials have aroused broad interest in various fields, such as electromagnetism [16,17] and acoustics [18,19]. For a two-dimensional case, highly anisotropic thermal conductivities happen to have adaptive responses to environmental changes [20,21], just like chameleons. We then perform coordinate transformations based on transformation-invariant metamaterials, which can keep the chameleonlike behavior. Therefore, the designed devices have adaptive responses to environmental changes. We take thermal rotators [22–26] as an example, which can guide the direction of heat flux. Existing designs are only applicable for a certain environment, which cannot cope with environmental changes. To improve the intelligence, we propose the concept of thermal chameleonlike rotators. Going beyond a normal isotropic shell with near-zero thermal conductivity [see Fig. 1(a)], we start the rotation transformation from a transformation-invariant shell [see Fig. 1(b)]. In this way, the designed rotator can adaptively work in different environments [see Figs. 1(c) and 1(d)], thus called a chameleonlike rotator. The environment denotes the

*13307110076@fudan.edu.cn
†jphuang@fudan.edu.cn

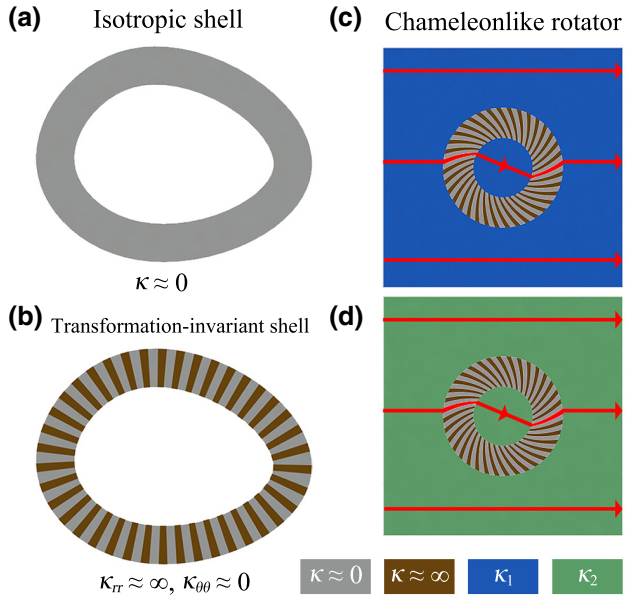

FIG. 1. Schematic diagram of thermal chameleonlike rotator. (a) Isotropic shell with near-zero thermal conductivity. (b) Transformation-invariant shell with near-zero thermal conductivity in tangential direction and near-infinite thermal conductivity in radial direction. (c),(d) Thermal chameleonlike rotator working in different environments. Lines with arrows indicate heat flow. The environmental thermal conductivities of (c),(d) are κ_1 and κ_2, respectively.

regions except the rotator, and the environmental parameter refers to the thermal conductivity. The scheme is further validated by simulations and experiments. Let us start from the theory.

II. THEORETICAL METHODS

We consider a passive and stable conduction process in two dimensions, which is governed by the Fourier law,

$$\nabla \cdot \left(- \overleftrightarrow{\kappa} \cdot \nabla T \right) = 0. \tag{1}$$

The whole system is divided into three regions, i.e., core, shell, and background, with tensorial thermal conductivities of $\overleftrightarrow{\kappa}_1 = \kappa_1 \overleftrightarrow{I}$, $\overleftrightarrow{\kappa}_2 = \mathrm{diag}\,(\kappa_{rr}, \kappa_{\theta\theta})$, and $\overleftrightarrow{\kappa}_3 = \kappa_3 \overleftrightarrow{I}$, respectively. We treat the core and background as the environment, and suppose their thermal conductivities to be the same, i.e., $\kappa_1 = \kappa_3$. $\overleftrightarrow{\kappa}_2$ is expressed in cylindrical coordinates (r, θ). By solving the Laplace equation, the effective thermal conductivity of the core and shell κ_e can be expressed as

$$\kappa_e = \kappa_{rr} \frac{n_1 \left(\kappa_1 - n_2 \kappa_{rr}\right) - n_2 \left(\kappa_1 - n_1 \kappa_{rr}\right) p^{(n_1 - n_2)/2}}{\kappa_1 - n_2 \kappa_{rr} - \left(\kappa_1 - n_1 \kappa_{rr}\right) p^{(n_1 - n_2)/2}}, \tag{2}$$

where $n_{1,2} = \pm\sqrt{\kappa_{\theta\theta}/\kappa_{rr}}$ and $p = (R_1/R_2)^2$. R_1 and R_2 are the inner and outer radii of the shell, respectively. The thermal conductivity of a transformation-invariant metamaterial is

$$\overleftrightarrow{\kappa}_2 = \begin{pmatrix} \infty & 0 \\ 0 & 0 \end{pmatrix}. \tag{3}$$

The substitution of Eq. (3) into Eq. (2) yields

$$\kappa_e \approx \kappa_1, \tag{4}$$

which means that the effective thermal conductivity of the core-shell structure can adaptively change with the environment. In other words, two-dimensional transformation-invariant metamaterials [Eq. (3)] have a chameleonlike behavior [Eq. (4)].

We then consider an arbitrary two-dimensional coordinate transformation,

$$r' = R\,(r,\, \theta)\,, \tag{5a}$$

$$\theta' = \Theta\,(r, \theta)\,, \tag{5b}$$

where $(r',\, \theta')$ are physical coordinates and $(r,\, \theta)$ are virtual coordinates. We can express the Jacobian matrix $\mathbf{J}$ as

$$\mathbf{J} = \begin{pmatrix} \dfrac{\partial r'}{\partial r} & \dfrac{\partial r'}{r \partial \theta} \\ \dfrac{r' \partial \theta'}{\partial r} & \dfrac{r' \partial \theta'}{r \partial \theta} \end{pmatrix}. \tag{6}$$

The transformed thermal conductivity is

$$\overleftrightarrow{\kappa}'_2 = \frac{\mathbf{J}\, \overleftrightarrow{\kappa}_2\, \mathbf{J}^{\mathrm{T}}}{\det \mathbf{J}}, \tag{7}$$

which can be expressed in detail as

$$\overleftrightarrow{\kappa}'_2 = \frac{1}{\det \mathbf{J}} \begin{bmatrix} \kappa_{rr} \left(\dfrac{\partial r'}{\partial r}\right)^2 + \kappa_{\theta\theta} \left(\dfrac{\partial r'}{r \partial \theta}\right)^2 & \kappa_{rr} \left(\dfrac{\partial r'}{\partial r}\right) \left(\dfrac{r' \partial \theta'}{\partial r}\right) + \kappa_{\theta\theta} \left(\dfrac{\partial r'}{r \partial \theta}\right) \left(\dfrac{r' \partial \theta'}{r \partial \theta}\right) \\ \kappa_{rr} \left(\dfrac{\partial r'}{\partial r}\right) \left(\dfrac{r' \partial \theta'}{\partial r}\right) + \kappa_{\theta\theta} \left(\dfrac{\partial r'}{r \partial \theta}\right) \left(\dfrac{r' \partial \theta'}{r \partial \theta}\right) & \kappa_{rr} \left(\dfrac{r' \partial \theta'}{\partial r}\right)^2 + \kappa_{\theta\theta} \left(\dfrac{r' \partial \theta'}{r \partial \theta}\right)^2 \end{bmatrix}. \tag{8}$$

With Eq. (3), the eigenvalues of Eq. (8) are

$$\lambda_1 = \frac{\kappa_{rr}}{\det \mathbf{J}}\left[\left(\frac{\partial r'}{\partial r}\right)^2 + \left(\frac{r'\partial\theta'}{\partial r}\right)^2\right], \tag{9a}$$

$$\lambda_2 \approx \frac{\kappa_{\theta\theta}}{\det \mathbf{J}}. \tag{9b}$$

Due to $\kappa_{rr} = \infty$ and $\kappa_{\theta\theta} = 0$, Eq. (9) can be further reduced to

$$\lambda_1 = \infty, \tag{10a}$$

$$\lambda_2 = 0. \tag{10b}$$

Clearly, an arbitrary coordinate transformation does not change the eigenvalues.

We then design a thermal chameleonlike rotator with transformation-invariant metamaterials. The coordinate transformation of rotating can be expressed as

$$r' = r, \tag{11a}$$

$$\theta' = \theta + \theta_0 \quad (r < R_1), \tag{11b}$$

$$\theta' = \theta + \theta_0 (R_2 - r) / (R_2 - R_1) \quad (R_1 < r < R_2), \tag{11c}$$

where θ_0 is rotation angle. With Eqs. (6) and (7), we can derive the thermal conductivity of the rotator as

$$\overleftrightarrow{\kappa}_2' = \begin{bmatrix} \kappa_{rr} & \kappa_{rr}\dfrac{r'\theta_0}{R_2 - R_1} \\ \kappa_{rr}\dfrac{r'\theta_0}{R_2 - R_1} & \kappa_{rr}\left(\dfrac{r'\theta_0}{R_2 - R_1}\right)^2 + \kappa_{\theta\theta} \end{bmatrix}, \tag{12}$$

which is the key parameter for a thermal chameleonlike rotator as long as $\overleftrightarrow{\kappa}_2$ satisfies Eq. (3).

III. SIMULATIONS AND EXPERIMENTS

To verify the scheme, we firstly perform simulations with COMSOL Multiphysics [27]. The system is the same as that in Fig. 1(c). We compare the difference between a chameleonlike rotator and a normal rotator (see Fig. 2). Before performing the rotation transformation, the thermal conductivities for the chameleonlike rotator and normal rotator are diag $(10^6, 10^{-3})$ and 100 W m^{-1} K^{-1}, respectively. The radial thermal conductivity of the transformation-invariant metamaterial should be much larger than the environmental thermal conductivity (at least 2 orders of magnitude), or the chameleonlike rotator may fail. We then change the environmental thermal conductivity from 10 to 1000 W m^{-1} K^{-1}, and the chameleonlike rotator can always work, i.e., rotating heat flux without distorting the environmental temperature profile [see Figs. 2(a)–2(c)]. Therefore, the simulation results confirm the chameleonlike property. However, the normal

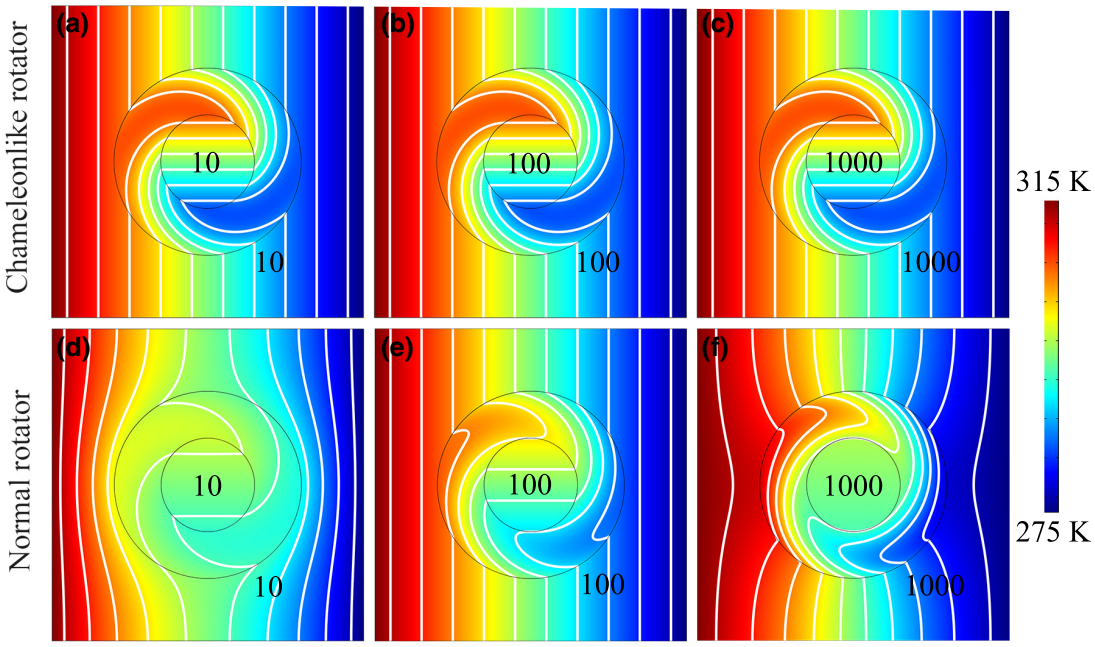

FIG. 2. Simulation results of (a)–(c) chameleonlike rotator and (d)–(f) normal rotator. White lines represent isotherms, and the values in each simulation are the corresponding thermal conductivities. The system size is 1×1 m^2. The outer and inner diameters of the shell are 0.3 and 0.6 m, respectively.

rotator fails. When the environmental thermal conductivity is $100\,\mathrm{W\,m^{-1}\,K^{-1}}$, it behaves as a traditional rotator [see Fig. 2(e)]. When the environment changes, the temperature profile is distorted [see Figs. 2(d) and 2(f)]. Therefore, the normal rotator has no response to environmental changes.

For experimental verification, it is difficult to find a material in nature that satisfies Eq. (12). Therefore, we use the effective medium theory to realize the corresponding parameter. Drawing on the multilayered structure [22], we design the chameleonlike rotator as shown in Fig. 3(a). As required by Eqs. (3) and (12), we choose two materials with extremely large ($\kappa_l \approx 10^6\,\mathrm{W\,m^{-1}\,K^{-1}}$) and extremely small ($\kappa_s \approx 10^{-3}\,\mathrm{W\,m^{-1}\,K^{-1}}$) thermal conductivities to approximately satisfy Eq. (3), and then use the helical structure to approximately satisfy Eq. (12). The simulation results are shown in Figs. 3(b)–3(g). Among them, Figs. 3(b)–3(d) show the results of chameleonlike rotator-1, rotating heat flux 90°. Figures 3(e) and 3(f) present the results of chameleonlike rotator-2, rotating heat flux 180°. Therefore, it is feasible to fabricate chameleonlike rotators with multilayered composite structures.

Limited by experimental conditions, we choose copper ($\kappa_{\mathrm{Cu}} \approx 400\,\mathrm{W\,m^{-1}\,K^{-1}}$) and air ($\kappa_{\mathrm{air}} \approx 0.026\,\mathrm{W\,m^{-1}\,K^{-1}}$) to fabricate a multilayered composite structure to realize a small-angle rotator. According to the series and parallel connection formula [28], the effective thermal conductivity of the composite structure is about $\mathrm{diag}\,(200,\ 0.052)\,\mathrm{W\,m^{-1}\,K^{-1}}$ before transformation. This puts a limit on the variation range of the environmental thermal conductivity. We calculate κ_e with κ_1 changing from 0.1 to $50\,\mathrm{W\,m^{-1}\,K^{-1}}$, and confirm that the chameleonlike rotator works well from 0.1 to $5\,\mathrm{W\,m^{-1}\,K^{-1}}$, as shown in Fig. 4(b). The difference $|\kappa_e - \kappa_1|$ is smaller than $0.05\,\mathrm{W\,m^{-1}\,K^{-1}}$ (denoted by the star, with a deviation smaller than 1%). Therefore, we conduct experiments with environmental thermal conductivities of 1 and $5\,\mathrm{W\,m^{-1}\,K^{-1}}$. The system is designed as shown in Fig. 4(a). The chameleonlike rotator is composed of air and copper, which is fabricated by laser cutting. The environment is colloidal materials obtained by mixing silica gel ($\kappa_{\mathrm{gel}} = 0.15\,\mathrm{W\,m^{-1}\,K^{-1}}$ and density $\rho_{\mathrm{gel}} = 1.14 \times 10^3\,\mathrm{Kg\,m^{-3}}$) and white copper powder ($\kappa_{\mathrm{WCu}} = 33\,\mathrm{W\,m^{-1}\,K^{-1}}$ and $\rho_{\mathrm{WCu}} = 8.65 \times 10^3\,\mathrm{Kg\,m^{-3}}$). The thermal conductivity of the mixture is determined by the Bruggeman formula [29],

$$p_{\mathrm{gel}}\frac{\kappa_{\mathrm{gel}} - \kappa_{\mathrm{mix}}}{\kappa_{\mathrm{gel}} + 2\kappa_{\mathrm{mix}}} + (1 - p_{\mathrm{gel}})\frac{\kappa_{\mathrm{WCu}} - \kappa_{\mathrm{mix}}}{\kappa_{\mathrm{WCu}} + 2\kappa_{\mathrm{mix}}} = 0, \quad (13)$$

where p_{gel} is the volume fraction of silica gel in the mixture. By setting $\kappa_{\mathrm{mix}} = 1$ or $5\,\mathrm{W\,m^{-1}\,K^{-1}}$, we can derive the composition ratio of silica gel, which helps us fabricate the colloidal materials. Although interface thermal conductance [30,31] exists, the mixture of regions I and III has a little fluidity, which can ensure a good contact between the object and copper. We then fill two tanks with hot and ice water to act as hot and cold sources, respectively. The temperature profile of the sample is measured by the FLIR E60 infrared camera. The experimental results are shown in Figs. 4(d) ($\kappa_{\mathrm{mix}} = 1\,\mathrm{W\,m^{-1}\,K^{-1}}$) and 4(f) ($\kappa_{\mathrm{mix}} = 5\,\mathrm{W\,m^{-1}\,K^{-1}}$). The corresponding simulation

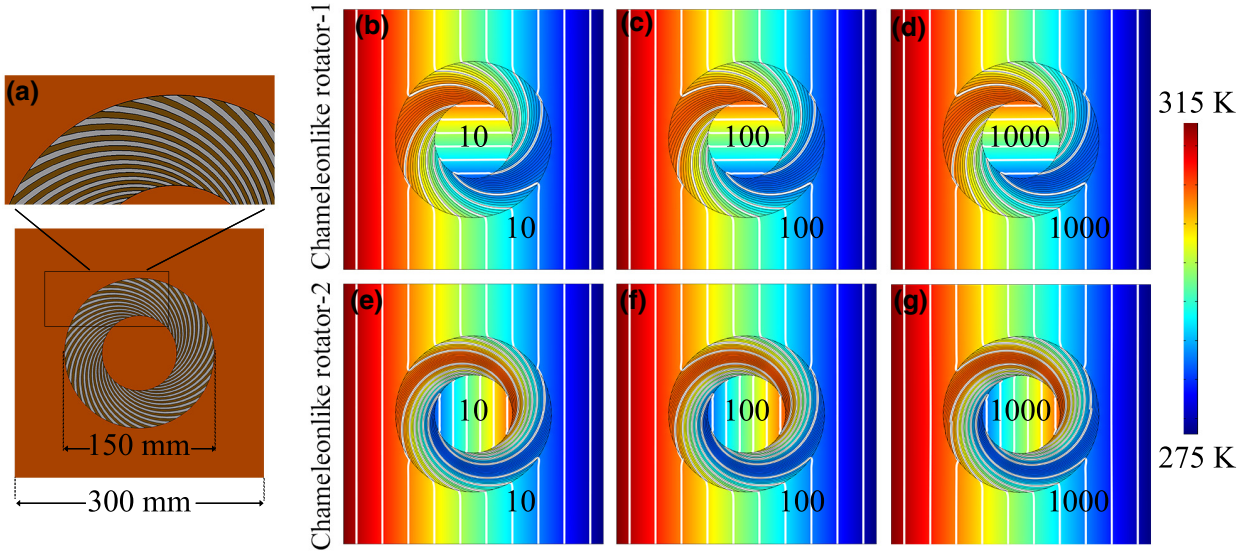

FIG. 3. Simulation results of chameleonlike rotators with multilayered structures. (a) Schematic diagram. The structure is composed of two kinds of materials with thermal conductivities of 10^6 and $10^{-3}\,\mathrm{W\,m^{-1}\,K^{-1}}$, respectively. Simulations results of (b)–(d) chameleonlike rotator-1 and (e)–(g) chameleonlike rotator-2 in different environments. The composite materials in (b)–(g) are the same as those in (a).

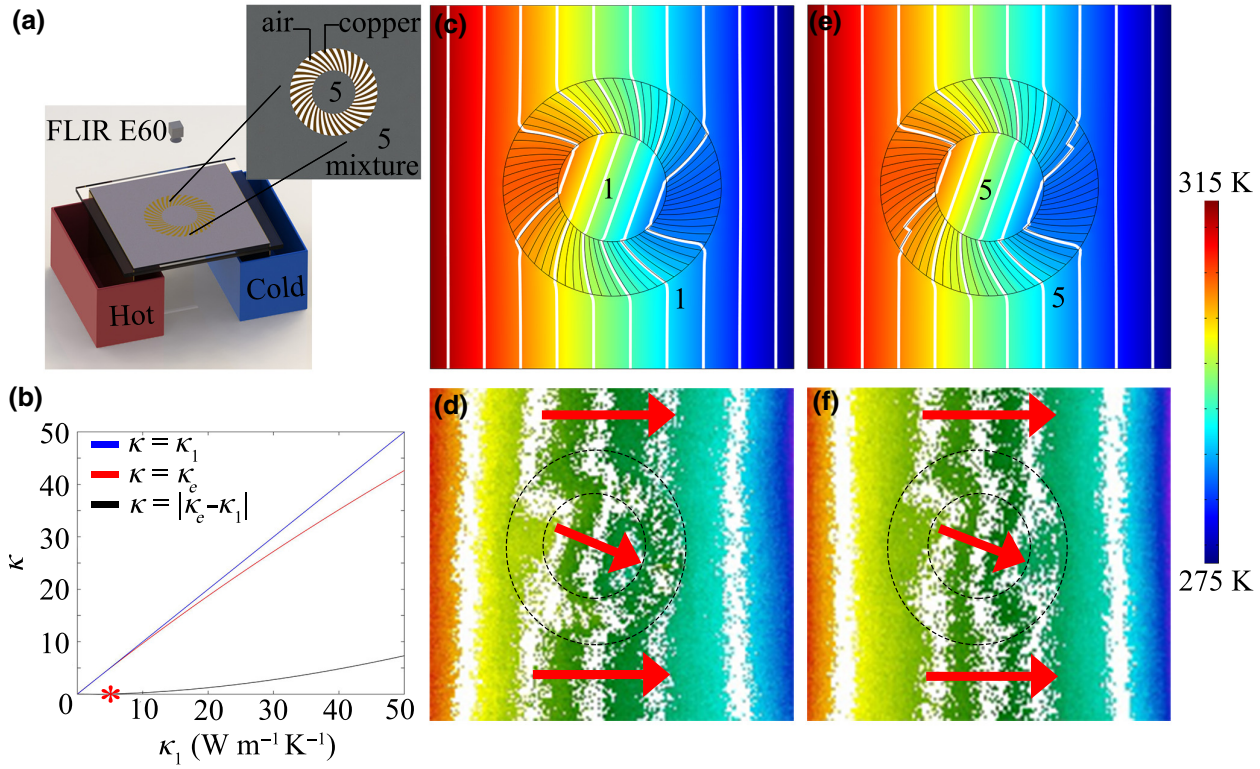

FIG. 4. Laboratory experiments of chameleonlike rotator. (a) Experimental setup. The structure is composed of copper ($\kappa_{Cu} \approx 400\,W\,m^{-1}\,K^{-1}$) and air ($\kappa_{air} \approx 0.026\,W\,m^{-1}\,K^{-1}$). (b) κ as a function of κ_1. The blue (top) and red (middle) lines correspond to κ_1 and κ_e, respectively. The black (bottom) line refers to $|\kappa_e - \kappa_1|$. The coordinate of $*$ is (5, 0.047). (c),(e) Simulation results and (d),(f) experimental results of the samples. The arrows indicate the direction of heat flux. The inner and outer diameters of the shell are 0.075 and 0.15 m, respectively.

results are presented in Figs. 4(c) and 4(e). Since the sample is connected to the hot and cold tanks with two copper plates, heat dissipation exists in the process. Moreover, the natural convection between the sample and air also results in heat dissipation. Therefore, there is a small difference between the computational and experimental values, but this does not affect the expected results. The isotherms still keep straight even though the environmental thermal conductivity changes. Meanwhile, heat flux is rotated as expected. Therefore, the experimental results are basically consistent with the simulation results, verifying the feasibility of chameleonlike rotators.

IV. DISCUSSION AND CONCLUSION

The major difference of our scheme is to start the coordinate transformation from a highly anisotropic parameter, which is proved to have a chameleonlike behavior. Therefore, the designed rotator based on this parameter can also have a chameleonlike behavior. Meanwhile, no matter how the shape of the rotator changes, the chameleonlike behavior still exists. Therefore, the present scheme can also design chameleonlike rotators with arbitrary shapes. Nevertheless, a perfect transformation-invariant (i.e., highly anisotropic) shell is described by Eq. (3), indicating that the higher anisotropy yields the better chameleonlike behavior and the wider working range. Due to the lack of highly conductive materials, the working range of the fabricated rotator is from 0.1 to 5 $W\,m^{-1}\,K^{-1}$. To improve the performance, more methods [32–36] can be applied to enhance thermal conductivities.

Moreover, the scheme can be extended to transient regimes by taking density and heat capacity into account [23,37–42]. The scheme is also not limited to conductive systems. Recent studies explored convective-diffusive systems [43–45], hydrodynamic systems [46,47], and acoustic systems [18,19] to design functional devices. Therefore, it is also promising to design chameleonlike rotators in these fields. Although these results are obtained at the macroscopic scale described the Fourier law, intelligence maybe also helpful for heat manipulations with nanostructures [48,49].

In conclusion, we propose the concept of chameleonlike rotators with transformation-invariant metamaterials. With a highly anisotropic thermal conductivity, the designed rotator can work in different environments, which saves time and labor. Both simulations and experiments verify the feasibility of the scheme. These results improve the

intelligence of traditional thermal metamaterials, and have potential applications in designing intelligent metamaterials. The proposed scheme can also be extended to other fields such as hydrodynamics, where the key parameter (permeability or viscosity) plays the similar role as thermal conductivity in thermotics.

ACKNOWLEDGMENTS

We acknowledge financial support from the National Natural Science Foundation of China under Grants No. 11725521 and No. 12035004, and from the Science and Technology Commission of Shanghai Municipality under Grant No. 20JC1414700.

[1] C. Z. Fan, Y. Gao, and J. P. Huang, Shaped graded materials with an apparent negative thermal conductivity, Appl. Phys. Lett. **92**, 251907 (2008).

[2] T. Y. Chen, C.-N. Weng, and J.-S. Chen, Cloak for curvilinearly anisotropic media in conduction, Appl. Phys. Lett. **93**, 114103 (2008).

[3] J. P. Huang, *Theoretical Thermotics: Transformation Thermotics and Extended Theories for Thermal Metamaterials* (Springer, Singapore, 2020).

[4] S. Guenneau, D. Petiteau, M. Zerrad, C. Amra, and T. Puvirajesinghe, Transformed Fourier and Fick equations for the control of heat and mass diffusion, AIP Adv. **5**, 053404 (2015).

[5] G. L. Dai, J. Shang, and J. P. Huang, Theory of transformation thermal convection for creeping flow in porous media: Cloaking, concentrating, and camouflage, Phys. Rev. E **97**, 022129 (2018).

[6] L. J. Xu and J. P. Huang, Controlling thermal waves with transformation complex thermotics, Int. J. Heat Mass Transf. **159**, 120133 (2020).

[7] L. J. Xu, G. L. Dai, and J. P. Huang, Transformation Multithermotics: Controlling Radiation and Conduction Simultaneously, Phys. Rev. Appl. **13**, 024063 (2020).

[8] L. J. Xu, S. Yang, G. L. Dai, and J. P. Huang, Transformation omnithermotics: Simultaneous manipulation of three basic modes of heat transfer, ES Energy Environ. **7**, 65 (2020).

[9] R. G. Peng, Z. Q. Xiao, Q. Zhao, F. L. Zhang, Y. G. Meng, B. Li, J. Zhou, Y. C. Fan, P. Zhang, N.-H. Shen, T. Koschny, and C. M. Soukoulis, Temperature Controlled Chameleonlike Cloak, Phys. Rev. X **7**, 011033 (2017).

[10] Y. Li, X. Bai, T. Z. Yang, H. L. Luo, and C.-W. Qiu, Structured thermal surface for radiative camouflage, Nat. Commun. **9**, 273 (2018).

[11] Y. C. Liu, F. Sun, and S. L. He, Fast adaptive thermal buffering by a passive open shell based on transformation thermodynamics, Adv. Theory Simul. **1**, 1800026 (2018).

[12] F. Sun, Y. H. Liu, Y. B. Yang, Z. H. Chen, and S. L. He, Thermal surface transformation and its applications to heat flux manipulations, Opt. Express **27**, 33757 (2019).

[13] N. Athanasopoulos and N. J. Siakavellas, Heat manipulation using highly anisotropic pitch-based carbon fiber composites, Adv. Engin. Mater. **17**, 1494 (2015).

[14] J. Y. Wan, J. W. Song, Z. Yang, D. Kirsch, C. Jia, R. Xu, J. Q. Dai, M. W. Zhu, L. S. Xu, C. J. Chen, Y. B. Wang, Y. L. Wang, E. Hitz, S. D. Lacey, Y. F. Li, B. Yang, and L. B. Hu, Highly anisotropic conductors, Adv. Mater. **29**, 1703331 (2017).

[15] A. Hamed and S. Ndao, High anisotropy metamaterial heat spreader, Int. J. Heat Mass Transf. **121**, 10 (2018).

[16] Y. M. Zhang and B. L. Zhang, Bending, splitting, compressing and expanding of electromagnetic waves in infinitely anisotropic media, J. Opt. **20**, 014001 (2018).

[17] Y. M. Zhang, Y. Luo, J. B. Pendry, and B. L. Zhang, Transformation-Invariant Metamaterials, Phys. Rev. Lett. **123**, 067701 (2019).

[18] L. T. Wu, M. Oudich, W. K. Cao, H. L. Jiang, C. Zhang, J. C. Ke, J. Yang, Y. C. Deng, Q. Cheng, T. J. Cui, and Y. Jing, Routing Acoustic Waves via a Metamaterial with Extreme Anisotropy, Phys. Rev. Appl. **12**, 044011 (2019).

[19] M. H. Fakheri, A. Abdolali, and H. B. Sedeh, Arbitrary Shaped Acoustic Concentrators Enabled by Null Media, Phys. Rev. Appl. **13**, 034004 (2020).

[20] L. J. Xu, S. Yang, and J. P. Huang, Passive Metashells with Adaptive Thermal Conductivities: Chameleonlike Behavior and its Origin, Phys. Rev. Appl. **11**, 054071 (2019).

[21] L. J. Xu and J. P. Huang, Chameleonlike metashells in microfluidics: A passive approach to adaptive responses, Sci. China-Phys. Mech. Astron. **63**, 228711 (2020).

[22] S. Narayana and Y. Sato, Heat Flux Manipulation with Engineered Thermal Materials, Phys. Rev. Lett. **108**, 214303 (2012).

[23] S. Guenneau and C. Amra, Anisotropic conductivity rotates heat fluxes in transient regimes, Opt. Express **21**, 6578 (2013).

[24] L. J. Xu, S. Yang, and J. P. Huang, Thermal theory for heterogeneously architected structure: Fundamentals and application, Phys. Rev. E **98**, 052128 (2018).

[25] L. L. Zhou, S. Y. Huang, M. Wang, R. Hu, and X. B. Luo, While rotating while cloaking, Phys. Lett. A **383**, 759 (2019).

[26] Y.-L. Tsai, J. Y. Li, and T. Y. Chen, Simultaneous focusing and rotation of a bifunctional thermal metamaterial with constant anisotropic conductivity, J. Appl. Phys. **126**, 095103 (2019).

[27] http://www.comsol.com/.

[28] R. Z. Wang, L. J. Xu, and J. P. Huang, Thermal imitators with single directional invisibility, J. Appl. Phys. **122**, 215107 (2017).

[29] J. Shang, B. Y. Tian, C. R. Jiang, and J. P. Huang, Digital thermal metasurface with arbitrary infrared thermogram, Appl. Phys. Lett. **113**, 261902 (2018).

[30] J. Y. Li, Y. Gao, and J. P. Huang, A bifunctional cloak using transformation media, J. Appl. Phys. **108**, 074504 (2010).

[31] D. K. Ma, G. Zhang, and L. F. Zhang, Interface thermal conductance between β-Ga_2O^3 and different substrates, J. Phys. D: Appl. Phys. **53**, 434001 (2020).

[32] Y. Li, K.-J. Zhu, Y.-G. Peng, W. Li, T. Z. Yang, H.-X. Xu, H. Chen, X.-F. Zhu, S. H. Fan, and C.-W. Qiu, Thermal meta-device in analogue of zero-index photonics, Nat. Mater. **18**, 48 (2019).

[33] S. Yang, L. J. Xu, and J. P. Huang, Metathermotics: Nonlinear thermal responses of core-shell metamaterials, Phys. Rev. E **99**, 042144 (2019).

[34] L. J. Xu, S. Yang, and J. P. Huang, Effectively infinite thermal conductivity and zero-index thermal cloak, EPL **131**, 24002 (2020).
[35] J. X. Li, Y. Li, W. Y. Wang, L. Q. Li, and C.-W. Qiu, Effective medium theory for thermal scattering off rotating structures, Opt. Express **28**, 25894 (2020).
[36] J. X. Li, Y. Li, P.-C. Cao, T. Z. Yang, X.-F. Zhu, W. Y. Wang, and C.-W. Qiu, A continuously tunable solid-like convective thermal metadevice on the reciprocal line, Adv. Mater. **32**, 2003823 (2020).
[37] Y. G. Ma, L. Lan, W. Jiang, F. Sun, and S. L. He, A transient thermal cloak experimentally realized through a rescaled diffusion equation with anisotropic thermal diffusivity, NPJ Asia Mater. **5**, e73 (2013).
[38] T. Z. Yang, Y. Su, W. Xu, and X. D. Yang, Transient thermal camouflage and heat signature control, Appl. Phys. Lett. **109**, 121905 (2016).
[39] Y. X. Liu, W. L. Guo, and T. C. Han, Arbitrarily polygonal transient thermal cloaks with natural bulk materials in bilayer configurations, Int. J. Heat Mass Transf. **115**, 1 (2017).
[40] X. He, T. Z. Yang, X. W. Zhang, L. Z. Wu, and X. Q. He, Transient experimental demonstration of an elliptical thermal camouflage device, Sci. Rep. **7**, 16671 (2017).
[41] T. C. Han, P. Yang, Y. Li, D. Y. Lei, B. W. Li, K. Hippalgaonkar, and C.-W. Qiu, Full-parameter omnidirectional thermal metadevices of anisotropic geometry, Adv. Mater. **30**, 1804019 (2018).
[42] S. Y. Huang, J. W. Zhang, M. Wang, W. Lan, R. Hu, and X. B. Luo, Macroscale thermal diode-like black box with high transient rectification ratio, ES Energy Environ. **6**, 51 (2019).
[43] F. B. Yang, L. J. Xu, and J. P. Huang, Thermal illusion of porous media with convection-diffusion process: Transparency, concentrating, and cloaking, ES Energy Environ. **6**, 45 (2019).
[44] W.-S. Yeung, V.-P. Mai, and R.-J. Yang, Cloaking: Controlling Thermal and Hydrodynamic Fields Simultaneously, Phys. Rev. Appl. **13**, 064030 (2020).
[45] L. J. Xu and J. P. Huang, Negative thermal transport in conduction and advection, Chin. Phys. Lett. **37**, 080502 (2020).
[46] J. Park, J. R. Youn, and Y. S. Song, Hydrodynamic Metamaterial Cloak for Drag-Free Flow, Phys. Rev. Lett. **123**, 074502 (2019).
[47] J. Park, J. R. Youn, and Y. S. Song, Fluid-Flow Rotator Based on Hydrodynamic Metamaterial, Phys. Rev. Appl. **12**, 061002 (2019).
[48] D. K. Ma, X. Wan, and N. Yang, Unexpected thermal conductivity enhancement in pillared graphene nanoribbon with isotopic resonance, Phys. Rev. B **98**, 245420 (2018).
[49] H. Bao, J. Chen, X. K. Gu, and B. Y. Cao, A review of simulation methods in micro/nanoscale heat conduction, ES Energy Environ. **1**, 16 (2018).